Chromium removal from electroplating wastewater by coir pith

Parinda Suksabye [a], Paitip Thiravetyan [b,*], Woranan Nakbanpote [c], Supanee Chayabutra [d]

[a] *The Joint School of Energy and Environment, King Mongkut's University of Technology Thonburi, 91 Pracha-Utit Road, Bangmod, Thungkru, Bangkok 10140, Thailand*
[b] *Division of Biotechnology, School of Bioresources and Technology, King Mongkut's University of Technology Thonburi, 83 Moo. 8 Thakham, Bangkhuntien, Bangkok 10150, Thailand*
[c] *Pilot Plant Development and Training Institute, King Mongkut's University of Technology Thonburi, 83 Moo. 8 Thakham, Bangkhuntien, Bangkok 10150, Thailand*
[d] *Department of Chemistry, Faculty of Science, Silpaorn University, 6 Rajamankhanai Road, Amphoe Muang, Nakorn Pathom Province, Bangkok 73000, Thailand*

Abstract

Coir pith is a by-product from padding used in mattress factories. It contains a high amount of lignin. Therefore, this study investigated the use of coir pith in the removal of hexavalent chromium from electroplating wastewater by varying the parameters, such as the system pH, contact time, adsorbent dosage, and temperature. The maximum removal (99.99%) was obtained at 2% (w/v) dosage, particle size <75 μm, at initial Cr(VI) 1647 mg l^{-1}, system pH 2, and an equilibrium time of 18 h. The adsorption isotherm of coir pith fitted reasonably well with the Langmuir model. The maximum Cr(VI) adsorption capacity of coir pith at 15, 30, 45 and 60 °C was 138.04, 197.23, 262.89 and 317.65 mg Cr(VI) g^{-1} coir pith, respectively. Thermodynamic parameters indicated an endothermic process and the adsorption process was favored at high temperature. Desorption studies of Cr(VI) on coir pith and X-ray absorption near edge structure (XANES) suggested that most of the chromium bound on the coir pith was in Cr(III) form due to the fact that the toxic Cr(VI) adsorbed on the coir pith by electrostatic attraction was easily reduced to less toxic Cr(III). Fourier transform infrared (FT-IR) spectrometry analysis indicated that the carbonyl (C=O) groups and methoxy (O–CH$_3$) groups from the lignin structure in coir pith may be involved in the mechanism of chromium adsorption. The reduced Cr(III) on the coir pith surface may be bound with C=O groups and O–CH$_3$ groups through coordinate covalent bonding in which a lone pair of electrons in the oxygen atoms of the methoxy and carbonyl groups can be donated to form a shared bond with Cr(III).

1. Introduction

Presently, there are a great number of electroplating factories in Thailand, which are almost all small-medium enterprises (SME). The conventional method of chrome-plating is widely adopted (>95%) for electroplating in Bangkok [1]. Consequently, a large volume of chromium-contaminated wastewater is generated by electroplating industries. Therefore, it is necessary to treat the wastewater before being discharged into the aquatic system. A cost-effective alternative technology for the treatment of wastewater is highly desired by the industry, especially in developing countries like Thailand.

Chromium exits in natural water in two main oxidation states, hexavalent chromium, Cr(VI) and trivalent chromium, Cr(III) [2]. However, Cr(VI) is more hazardous, carcinogenic and mutagenic to living organisms [3]. In addition, it leads to liver damage, pulmonary congestion and causes skin irritation resulting in ulcer formation [4]. Cr(VI) is widely found in electroplating wastewater in which it is primarily present in the form of oxyanions, such as chromate (CrO$_4^{2-}$), dichromate (Cr$_2$O$_7^{2-}$), bichromate (HCrO$_4^-$) which are dependent on the pH and Cr(VI) concentration [5]. Because of its high toxicity, Cr(VI) must be substantially removed from the wastewater before being discharged into the aquatic system. The maximum Cr(VI) and Cr(III) levels that are permitted in industrial wastewater by the Ministry of Industry in Thailand are 0.25 and 0.75 mg l^{-1}, respectively.

* Corresponding author. Tel.: +66 2 4707535; fax: +66 2 4523455.
  E-mail address: paitip.thi@kmutt.ac.th (P. Thiravetyan).

The methods employed for the removal of Cr(VI) from wastewater include reduction, precipitation, reverse osmosis, ion exchange and electrodialysis [2,4,6,7]. However, these treatment methods are not widely practiced due to their high operation costs and problems in the disposal of the residual metal sludges [8]. Adsorption is an economically feasible alternative, which is effective and versatile in removing chromium, particularly when combined with appropriate regeneration steps [9]. The use of activated carbon as an adsorbent is still very popular and different grades are available, but are quite expensive [10]. Considerable research work has been done in the search for inexpensive adsorbents such as sawdust, sugar beet pulp, sugar cane bagasse and maize cob [11], hazelnut-shell activated carbon [4], wool, olive cake, pine needles, almond, charcoal and cactus leaves [9], rice husk carbon and activated alumina [8], Fe-modified steam wheat straw [6], *Caurina equisetifolia* leaves [7], activated carbon prepared from coconut tree sawdust [12], used tyres [13], soya cake [14], distillery sludge [15], coconut shell charcoal [5] and non-living *Eichhornia crassipes* (water hyacinth) [16]. However, some of these adsorbents do not contain high adsorption capacities.

Coir pith, light to dark brown in color, consists primarily of particles in the size range 0.2–4 mm. It is the by-product of coir fiber extraction from coconut husk used in mattress padding. It contains a high amount of lignin of 36% (data in this study). Thus, in this present study, coir pith was used as an adsorbent to investigate its potential for the removal of Cr(VI). It was found to not only reduce costs for wastewater treatment, but also to add value to the waste.

In this study, batch experiments were conducted to investigate the adsorption capacity and mechanism of Cr(VI) using coir pith. The effects of parameters such as the system pH, adsorbent dosage and contact time were examined. Fourier transformed infrared (FT-IR) spectrometry, X-ray absorption near edge structure (XANES) and desorption studies were investigated to confirm the mechanism of the Cr(VI) adsorption.

2. Methodology

2.1. Adsorbent preparation

Coir pith was obtained as a waste product from padding used in mattress factories in Prachuapkhirikhan province (Thailand). A commercial activated carbon based on coconut shell was obtained from Mazuma (Thailand) Co. Ltd. Both were dried in a hot air oven at 105 °C for 1 h and then crushed and sieved to obtain an approximate particle size less than 75 μm (−200 mesh, U.S standard sieve). In addition, α-cellulose, xylan from brickwood and xylan from oat spelt were obtained from S.M. Chemical Supplies Co. Ltd.

2.2. Electroplating wastewater

The chromium-contaminated wastewater was collected from an electroplating factory, located in Samuthprakarn province (Thailand).

2.3. Adsorbent characteristics

A scanning electron microscope connecting with electron dispersive X-ray spectroscopy (SEM/EDX) (JEOL, JSM-5800LV) was used to examine the surface morphologies and compositions of coir pith and activated carbon based on coconut shell (<75 μm).

The specific surface areas of the coir pith and activated carbon were determined by the BET method using a Surface Area Analyzer (Quantachrom, Autosorb-1, USA).

pH$_{zpc}$ (pH of zero point of charge) was determined with a different pH system by titration [17,18]. The coir pith was ground to <75 μm and dried at 105 °C for 4 h. A mixture of 0.2 g dried coir pith and 50 ml of deionised water (pH 7) was mixed with nitrogen gas for 15 min, and then shaken at 250 rpm, at 30 °C for 1 h. The pH was measured after an equilibrium time of 10 min with a pH meter. The titration was carried out with 0.1 M NaOH and 0.1 M HNO$_3$, respectively. The surface charge (Q) was calculated from the experimental titration data according to Eq. (1). The pH of zero point of charge ($Q = 0$) was obtained from the plot of Q versus pH:

$$Q = \frac{1}{w}(C_a - C_b - [\text{H}^+] + [\text{OH}^-]) \qquad (1)$$

where Q is the surface charge (mol g^{-1} adsorbent dry weight); C_a is the added acid (mol l^{-1}); C_b is the added base (mol l^{-1}); w is the adsorbent dry weight (g l^{-1}).

2.4. Effect of contact time

Batch experiments were carried out by placing 0.2 g of coir pith and 10 ml of electroplating wastewater in a 20 ml sealed glass bottle (2% (w/v)) and then agitating the mixtures at 150 rpm with varying contact times from 5 min to 24 h in a system pH of 2 at 30 °C. The adsorbent and adsorbate were separated by centrifugation at 4500 rpm for 10 min. Then, the Cr(VI) concentration remaining in the supernatant was measured using a spectrophotometer (Spectronic 21, BAUSCH & LOMB) through the development of a purple-violet color with 1,5-diphenyl carbazide in an acidic solution at a wavelength of 540 nm.

2.5. Effect of system pH

The effect of the system pH was studied, following the same procedure as for the contact time, over a system pH range from 2 to 10 adjusted with 1 M NaOH or 0.1 M H$_2$SO$_4$ after the addition of coir pith. Total chromium (Cr(VI) + Cr(III)) was also determined by Inductively Coupled Plasma Spectrometer (ICP), Jobin Yvon-JY 124, France. The difference in concentration between the total and hexavalent chromium (Cr(VI)) was taken as the concentration of trivalent chromium, Cr(III). In addition, the pH of the final treated wastewater was analyzed by a pH meter (Mettler delta 340, USA).

2.6. Effect of adsorbent dosage

The effect of the adsorbent dosage on the adsorption of Cr(VI) was studied by varying the coir pith dosage from 0.02 to 0.45 g in

10 ml of electroplating wastewater. The system pH was adjusted to 2.

2.7. Adsorption isotherm and effect of temperature

Experiments were conducted by varying the dosage of coir pith and activated carbon based on coconut shell in the range of 0.01–0.18 g and shaking with 10 ml of electroplating wastewater for 18 h at different temperatures (15, 30, 45, 60 °C). The system pH was adjusted to 2.

2.8. X-ray absorption near edge structure (XANES)

XANES was used to determine the oxidation state of chromium bound on the coir pith. The coir pith was loaded with 1481 mg l^{-1} Cr(VI) at system pH 2 for 18 h. The Cr(VI)-adsorbed coir pith from the adsorption process was ground with agate mortar and loaded into the sample plates with kapton tape for analysis at the National Synchrotron Research Center. The XANES studies of the samples were performed on beamline 8. The XANES data for chromium was collected with K edges and energy of 5.989 keV. The operating conditions for the beamline were a beam energy of 1.2 GeV, a current between 27 and 50 mA with an indium antimonide crystals monochromator, InSb(1 1 1). Chromium trioxide (CrO_3) and chromium(III) sulfate hydrate ($Cr_2(SO_4)_3 \cdot xH_2O$) were used as a Cr(VI) and Cr(III) standard, respectively.

2.9. Desorption study

A 1481 mg l^{-1} dose of Cr(VI) solution was adsorbed onto 2% (w/v) of coir pith and activated carbon and shaken at 150 rpm, at 30 °C for 18 h. The Cr(VI)-adsorbed sample was filtered and air-dried. The desorption study was carried out by agitating 0.2 g of Cr(VI)-adsorbed adsorbents with 10 ml of 0.1 M NaOH, 0.5 M NaOH, 1 M NaOH, 0.5 M HNO$_3$, 1 M HNO$_3$ and 2 M HNO$_3$ at 30 °C and shaken at 150 rpm for 24 h. Then, the sample was centrifuged and the supernatant was used to determine the percentage of chromium adsorption. In addition, Cr(III) desorbed in solution was oxidized to Cr(VI) with 1 M potassium persulphate ($K_2S_2O_8$) by using one part of Cr(III) solution and one part of 1 M $K_2S_2O_8$ (1:1, v/v). This mixed solution was heated at 100 °C.

2.10. Fourier transform infrared analysis (FT-IR)

For the adsorption process, samples of coir pith were loaded with 1481 mg l^{-1} of Cr(VI) at system pH 2. The samples of coir pith before and after Cr(VI) adsorption, were analyzed by a Fourier transform infrared spectrometer (FT-IR), Perkin-Elmer spectrum one. The spectra of the adsorbents were carried out by the KBr disc technique. The samples were milled and mixed with KBr at a ratio of 1 mg sample/100 mg KBr.

2.11. Lignin extracted from coir pith

The lignin extracted from the coir pith was determined by the TAPPI method (TAPPI T222 om-88) [19]. One grams coir pith (preparation by TAPPI T264 cm-97) was placed in a 100 ml beaker and 72% sulfuric acid (15 ml) was added. The mixture in the beaker was stirred in a bath at 20 ± 1 °C. After 2 h, the mixtures were transferred into a 1000 ml flask, rinsed and diluted with distilled water to 3% concentration of sulfuric acid (total volume of 575 ml). Then, the lignin was extracted by using a reflux condenser (the solution being boiled for 4 h). The mixture was filtered through a filtering crucible, and the obtained acid-insoluble lignin was washed with distilled water and dried in air.

Table 1
BET surface area of coir pith and activated carbon based on coconut shell

Adsorbent	BET surface area (m^2 g^{-1})	Total pore volume (cm^3 g^{-1})	Average pore diameter (Å)
Coir pith	7.42	0.0143	76.83
Activated carbon	1113	0.6236	22.41

3. Results and discussion

3.1. Coir pith characteristics

It could be seen from a scanning electron microscope with electron dispersive X-ray spectroscopy (SEM/EDX) that the surface of coir pith is smooth and contains a low number of pores. The chemical compositions of coir pith measured by SEM/EDX contained C 52.09%, O 46.20%, Cl 0.89% and K 0.82%. Coir pith contains mainly carbon and oxygen. In addition, coir pith has a low specific surface area (Table 1).

3.2. Effect of contact time

The effect of contact time on the batch experiment of 1647 mg l^{-1} Cr(VI) at 30 °C and system pH 2 is shown in Fig. 1. The results indicated that the removal of Cr(VI) was rapid within the first 5 min (73.59%), the adsorption rate thereafter gradually decreasing. The data submitted to analysis of variance and means separation, using Duncan's new multiple range test (DMRT), were not significantly different at $P \leq 0.05$ indicating that the Cr(VI) adsorption by coconut coir pith from 18 to 24 h was not different. This indicated that the Cr(VI) adsorption reached equilibrium at 18 h.
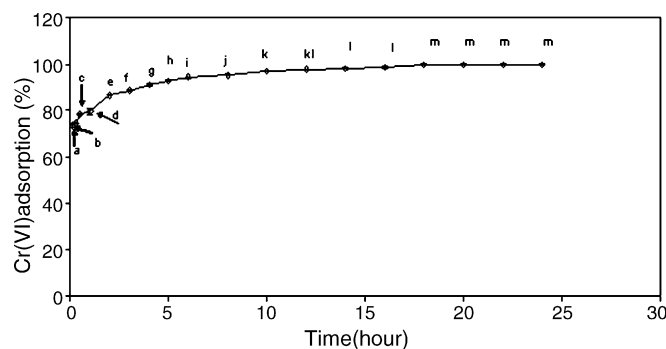

Fig. 1. Effect of contact time on Cr(VI) adsorption by coir pith (conditions: Cr(VI), 1647 mg l^{-1}; temperature, 30 °C; system pH, 2; dosage, 20 g l^{-1}; particle size, <75 μm).
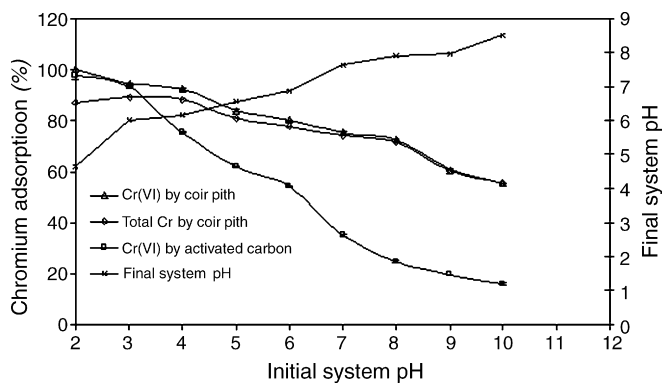
Fig. 2. Effect of system pH on chromium adsorption by coir pith and activated carbon based on coconut shell (conditions: total Cr, 1647 mg l^{-1}; Cr(VI), 1481 mg l^{-1}; temperature, 30 °C; contact time, 18 h; dosage, 20 g l^{-1}; particle size, <75 µm).

3.3. Effect of system pH

pH is the most important factor that controls the adsorption of Cr(VI). The effect of the system pH on Cr(VI) removal using coir pith is shown in Fig. 2. It is seen that the Cr(VI) adsorption efficiency decreases with the increase of the system pH values from 2 to 10. A similar trend can be observed for the Cr(VI) adsorption by activated carbon based on coconut shell (Fig. 2).

The maximum adsorption percentage on coir pith (99.99%) was observed at system pH 2. In addition, the removal percentage of total chromium was less than of Cr(VI) due to the fact that the direct reduction of Cr(VI) to Cr(III) in solution occurs at low pH values [8,11,20]. Therefore, the increased removal of Cr(VI) at low pH can be explained by the direct reduction of Cr(VI) to Cr(III) in solution and the electrostatic attraction between the Cr(VI) species and adsorbent surface [11]. The equation of Cr(VI) reduction is as below [20]:

$$HCrO_4^- + 7H^+ + 3e^- \Leftrightarrow Cr^{3+} + 4H_2O \quad E^0 = 1.20 \quad (2)$$
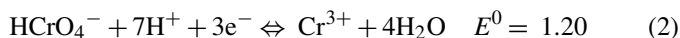
The pH $_{zpc}$ (zero point of charge) was found to be at 8.15 (Fig. 3) and below this pH (pH < 8.15), the surface charge of the adsorbent is positive. At pH 2 the predominant Cr(VI) was HCrO$_4^-$ [9,13], and therefore, electrostatic attraction occurred between the positively charged adsorbent and negatively charged HCrO$_4^-$. In contrast, the decrease in adsorption at higher pH values was apparently due to the competitiveness of the Cr(VI)
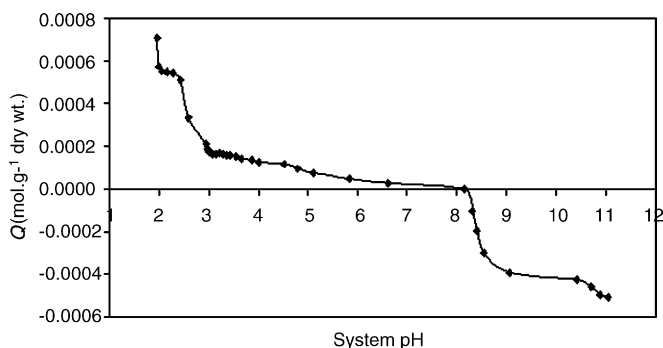
species (CrO$_4^{2-}$) and OH$^-$ ions in the bulk [21]. The adsorbent surface at pH > 8.15 is negatively charged. Thus, the electrostatic repulsion between the negatively charged Cr(VI) species and negatively charged adsorbent particles was increased. This led to a decease in the Cr(VI) adsorption.

In addition, it was found that the final system pH had increased from 2 to 4.64 after the adsorption reaction (Fig. 2) due to the fact that the direct reduction of Cr(VI) to Cr(III) to solution requires a large number of protons [20]. The increase in the final system pH was observed in all initial system pH values except pH 8–10. This can be explained in that the bichromate ions (HCrO$_4^-$) at higher pH solutions changed into chromate ions (CrO$_4^{2-}$) and released protons into the solution, as shown in Eq. (3) [22]. The release of hydrogen ions resulted in decreasing the final system pH:

$$HCrO_4^- \Leftrightarrow H^+ + CrO_4^{2-} \quad (\log K = -8) \quad (3)$$
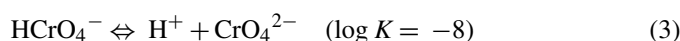
The occurrences of Cr(III) in the reduction of Cr(VI) to solution could not favorably be adsorbed on the coir pith at system pH 2 due to the electrostatic repulsion between Cr^{3+} and the positively charged coir pith (pH$_{zpc}$ < 8.15). This was confirmed by batch experiments of ordinary Cr(III) adsorption (CrCl$_3$·6H$_2$O) on coir pith. The results indicated that the adsorption capacities of Cr(III) on coir pith at system pH 2 was quite low (4.9 mg g^{-1}). Furthermore, Deng and Bai [23] reported that the optimum pH of Cr(III) adsorption on aminated polyacrylonitrile fiber was 6.5.

3.4. Effect of adsorbent dosage

The percentage adsorption of Cr(VI) was studied by increasing the adsorbent dosage from 2 to 45 g l^{-1} at 30 °C (Fig. 4). The adsorption efficiency generally improved with increasing adsorbent dosage up to a certain value and then remained constant. The data were submitted to analysis of variance and means separation was performed using Duncan's new multiple range test (DMRT). The results were not significantly different at $P \leq 0.05$ indicating that the Cr(VI) adsorption by coir pith from 20 to 45 g l^{-1} was not different. This indicated that the optimum dosage for Cr(VI) adsorption was 20 g l^{-1} at 99.99% of Cr(VI) adsorption. The
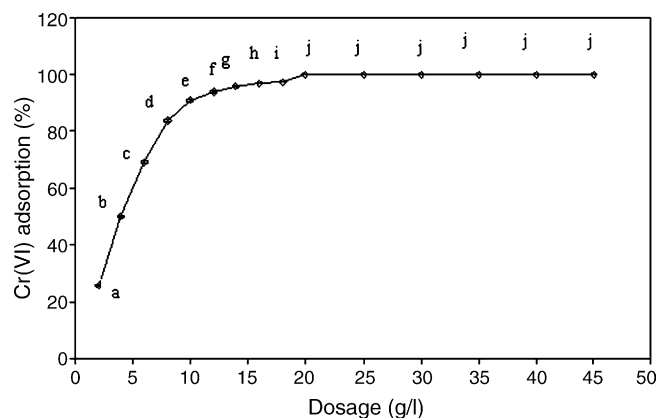

Fig. 4. Effect of adsorbent dosage on Cr(VI) adsorption by coir pith (conditions: Cr(VI), 1481 mg l^{-1}; temperature, 30 °C; contact time, 18 h; system pH, 2; particle size, <75 µm).

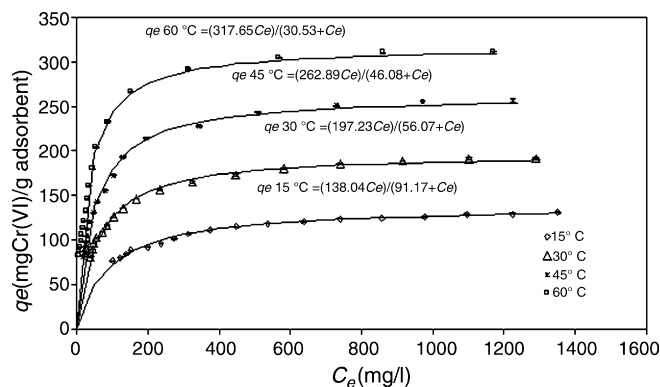Fig. 3. Variation of surface charge of coconut coir pith with system pH.

Fig. 5. Langmuir non-linear isotherm of Cr(VI) adsorption on coir pith at various temperatures (conditions: Cr(VI), $1481\,mg\,l^{-1}$; system pH, 2; contact time, 18 h; particle size, <75 μm).

increase in the adsorption percentage with increasing adsorbent dosage is due to the increase in the number of adsorbent sites (charging sites) [15].

3.5. Adsorption isotherms

Adsorption isotherms were used to describe the equilibrium established between adsorbed Cr(VI) on the coir pith (q_e) and Cr(VI) remaining in the solution (C_e) at constant temperature. The Langmuir equation refers to a monolayer sorption onto a surface containing a finite number of accessible sites [24]:

$$q_e = \frac{q_{max}bC_e}{1 + bC_e} \tag{4}$$

where q_{max} is the maximum quantity of Cr(VI) per unit weight of adsorbent to form a complete monolayer on the surface ($mg\,g^{-1}$); C_e the equilibrium concentration ($mg\,l^{-1}$); q_e the amount of Cr(VI) adsorbed at equilibrium ($mg\,g^{-1}$); b is the Langmuir constant related to energy of Cr(VI) adsorption ($l\,mg^{-1}$).

Adsorption isotherms at 15, 30, 45 and 60 °C were obtained at system pH 2 and an equilibrium time of 18 h by varying the adsorbent dosage in the range of $1–18\,g\,l^{-1}$. Fig. 5 shows the Langmuir non-linear isotherm of Cr(VI) adsorption by coir pith at the various temperatures of 15, 30, 45 and 60 °C, respectively. The calculated Langmuir constants are given in Table 2. The maximum adsorption capacity (q_{max}) of Cr(VI) increased

from 138.04 to $317.65\,mg\,g^{-1}$ with the increase of temperature from 15 to 60 °C. This behavior might be due to the increase in chemical interactions between the adsorbate ions and surface functionalities of adsorbent at higher temperatures. This is an endothermic process [25]. Similar to the Cr(VI) adsorption on commercial activated carbon based on coconut shell, the maximum Cr(VI) adsorption capacity increased from 137.61 to $302.80\,mg\,g^{-1}$ with increasing temperature from 15 to 60 °C (Table 2).

The Cr(VI) adsorption capacity on coir pith was $197.23\,mg\,g^{-1}$ at 30 °C, whereas that of activated carbon was only $185.01\,mg\,g^{-1}$ adsorbent under the same conditions; although activated carbon has a larger BET surface area than coir pith (Table 1). Furthermore, the adsorption capacity of coir pith is larger than that of sawdust ($15.82\,mg\,g^{-1}$) [9], almond ($10.62\,mg\,g^{-1}$) [9] and sulfuric acid-treated wheat bran ($104.17\,mg\,g^{-1}$) [25] and activated carbon developed from *Terminalia arjuna* nuts activated with zinc chloride ($28.43\,mg\,g^{-1}$) [26]. Therefore, the low cost coir pith has potential as a suitable adsorbent for the clean-up of chromium-contaminated wastewater.

The favorable nature of adsorption can be expressed in terms of a dimensionless parameter R_L, which is given by the following equation [15]:

$$R_L = \frac{1}{1 + bC_0} \tag{5}$$

where C_0 is the initial concentration ($mg\,l^{-1}$) and b is the Langmuir constant ($l\,mg^{-1}$). At all temperatures, R_L values were between 0 and 1 (Table 2), pointing to a favorable adsorption of Cr(VI) on coir pith.

The enthalpy change (ΔH) is calculated by the following equation:

$$\log b = \frac{-\Delta H}{2.303RT} + constant \tag{6}$$

where R is the gas constant ($8.314\,J\,mol^{-1}\,K^{-1}$), b the Langmuir constant ($l\,mg^{-1}$) and T is the temperature (K).

The enthalpy changes (ΔH) of Cr(VI) adsorption by coir pith and activated carbon determined from the slope of $\log b$ versus $1/T$ were found to be 33.39 and $33.44\,kJ\,mol^{-1}$, respectively. The positive value ΔH indicates the endothermic nature of the process.

Table 2
Langmuir constants for Cr(VI) adsorption by coir pith and activated carbon at various temperatures

Adsorbent	Temperature (°C)	Lamgmuir constants			
		q_{max} ($mg\,g^{-1}$)	b ($l\,mg^{-1}$)	r^2	R_L
Coir pith	15	138.04	0.011	0.996	0.058
	30	197.23	0.018	0.997	0.036
	45	262.89	0.022	0.995	0.030
	60	317.65	0.033	0.984	0.020
Activated carbon	15	137.61	0.007	0.999	0.089
	30	185.01	0.013	0.999	0.049
	45	246.16	0.016	0.997	0.038
	60	302.80	0.023	0.991	0.028

3.6. Desorption study

Desorption experiments were studied using 0.1 M NaOH, 0.5 M NaOH, 1 M NaOH and 0.5 M HNO₃, 1 M HNO₃, 2 M HNO₃ as eluents. The desorption values of Cr(VI) on coir pith using alkaline salts (0.1 M NaOH, 0.5 M NaOH, 1 M NaOH) were only 11.26–15.63%. On the other hand, the high desorption percentage on activated carbon based on coconut shell increased from 67.68% to 76.75% with the increase of the solution pH. In addition, 0.5 M HNO₃, 1 M HNO₃, 2 M HNO₃ were also used as eluents. About 38.12–71.48% of Cr(III) was desorbed by strong acid. The high Cr(III) and low Cr(VI) can be desorbed in acid and base solutions, respectively. This suggested that both Cr(VI) and Cr(III) still existed on the coir pith. Cr(III) bound on coir pith is easily desorbed by strong acid, and Cr(VI) bound on coir pith can be desorbed in the form of Cr(III) through reduction under strong acidic conditions [27].

However, it is possible to oxidize Cr(III) desorbed from coir pith to Cr(VI) for reuse in electroplating. Therefore, 1 M $K_2S_2O_8$ was used to oxidize Cr(III) to Cr(VI) and almost 100% of Cr(III) to change to Cr(VI). The equation is expressed as follows:

$$2Cr^{3+} + S_2O_8{}^{2-} + 6H_2O \overset{100\,^{\circ}C}{\Leftrightarrow} 2HCrO_4{}^{-} + 2HSO_3{}^{-} + 8H^{+}$$

(7)
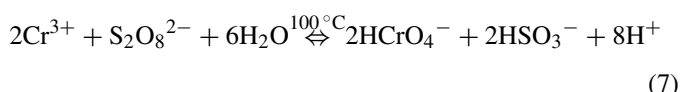
3.7. X-ray absorption near edge structure (XANES)

XANES was employed to confirm the oxidation state of chromium bound on the coir pith. Fig. 6 shows the XANES for Cr(VI) adsorbed coir pith at system pH 2. The XANES spectrum indicated that most of the Cr(III) species and part of the Cr(VI) were present on the coir pith. From this it might be concluded that most of the chromium bound on the coir pith was in Cr(III) form due to the fact that the toxicity of Cr(VI) bound on coir pith by electrostatic attraction is easily reduced to less toxic
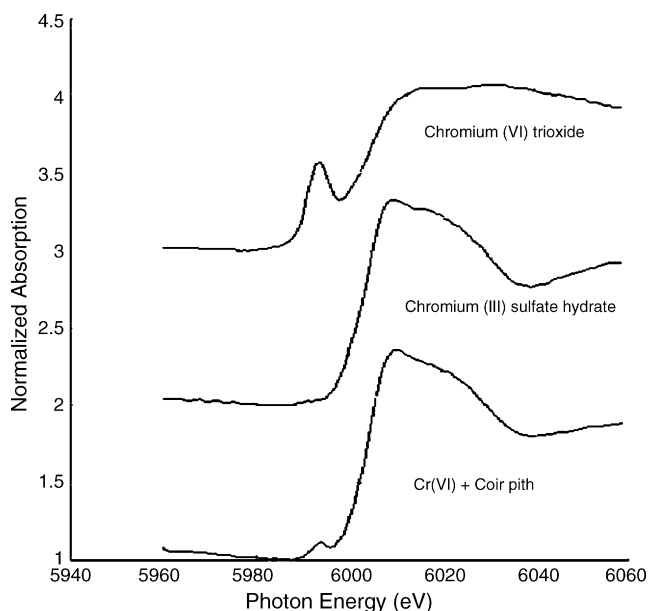
Cr(III) form [27–29]. However, the partial Cr(VI) still exists in the coir pith. This seems to indicate that the reduction of toxic Cr(VI) to less toxic Cr(III) on coir pith is still not complete. This study is similar to previous studies. Park et al. [27] reported that Cr(VI) can be favorably adsorbed with dead fugal biomass of *Aspergillus niger* at low pH. Their desorption and X-ray photoelectron spectroscopy (XPS) data presented that most of the chromium bound on adsorbent was in Cr(III) form due to the conversion of toxic Cr(VI) into less toxic Cr(III) on the adsorbent surface. Garsea-Torresdey et al. [29] reported that Cr(VI) could be bound on oat by-product by positively charged functional groups such as amine groups and subsequent reduction of toxic Cr(VI) to less toxic Cr(III).

3.8. FT-IR spectroscopy

The FT-IR spectra of coir pith, before and after Cr(VI) adsorption, are shown in Fig. 7. The FT-IR spectrum of coconut pith before adsorption reveals a broad peak around 3400 cm⁻¹ which can be attributed to the O–H group. The peak observed at 2921 cm⁻¹ corresponds to the C–H stretching group. In additional, there are many fingerprint regions between 1800 and 1000 cm⁻¹. These peaks are assigned to the carbonyl stretching group (C=O, 1735 cm⁻¹), C=C stretching of the aromatic ring vibration (1614, 1515 cm⁻¹), methoxy groups (O–CH₃, 1447 cm⁻¹) from lignin structure in the coir pith [30], O–H deformation originating from the phenolic group (1372, 1265 cm⁻¹), C–OH stretching in primary alcohol (1059 cm⁻¹) and secondary alcohol (1104 cm⁻¹). As illustrated in Fig. 7, the peak intensity of the carbonyl group was diminished in the FT-IR spectrum after Cr(VI) adsorption. Moreover, the peak intensity of the methoxy group was greatly decreased and shifted from 1447 to 1423 cm⁻¹. Therefore, it can be suggested that the carbonyl and methoxy groups from the lignin structure in coir pith may be involved in the mechanism of chromium adsorption.

In addition, FT-IR spectra of lignin extracted from coir pith, before and after Cr(VI) adsorption, were analyzed to confirm that the lignin in coir pith was involved in the Cr(VI) adsorption. As seen in Fig. 8, the O–CH₃ groups at 1447 cm⁻¹ also confirms that the lignin structures are contained in coir pith. The peak intensity of the carbonyl (1735 cm⁻¹) group disappeared and the

Fig. 6. XANES of coir pith after Cr(VI) adsorption at system pH 2.
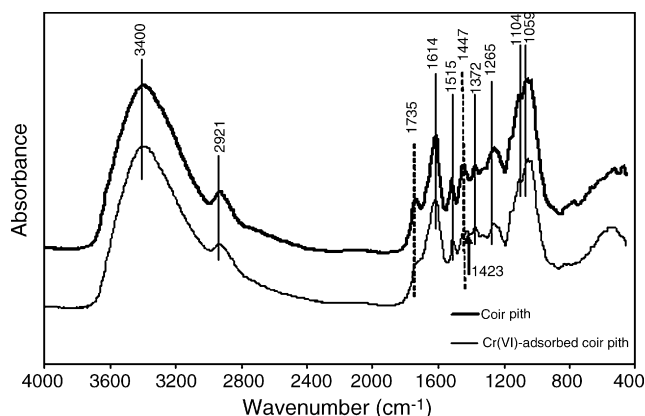

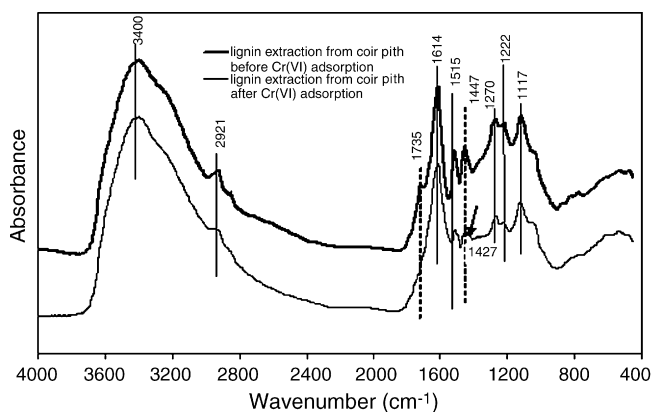Fig. 7. FT-IR spectrum of coir pith before and after Cr(VI) adsorption.

Fig. 8. FT-IR spectrum of lignin extracted from coir pith before and after Cr(VI) adsorption.

peak of the methoxy group was decreased and shifted from 1447 to 1427 cm^{-1}. Thus, it can be suggested that the carbonyl and methoxy groups may be involved in the mechanism of Cr(VI) adsorption.

To investigate if the lignin in coir pith may be involved in the mechanism of Cr(VI) adsorption, adsorption studies of Cr(VI) onto lignin extracted from coir pith, α-cellulose, xylan from brick wood and xylan from oat spelt were carried out in batch experiments under the same conditions. The results showed that the percentages of Cr(VI) adsorption on α-cellulose (8.14%), xylan from brick wood (16.49%) and xylan from oat spelt (24.36%) were low, while both lignin extracted from coir pith and coir pith itself were 100% of Cr(VI) adsorption. Therefore, it can be confirmed that lignin in coir pith was involved in chromium adsorption.

3.9. Mechanism of Cr(VI) adsorption by coir pith

In the present study, the maximum Cr(VI) removal on coir pith was obtained at system pH 2. The improved removal Cr(VI) at low pH was due to electrostatic attraction between negative charged $HCrO_4^-$ and positive charged coir pith and the direct reduction of Cr(VI) to Cr(III) in the solution. However, the occurrences of Cr(III) in the solution could not favorably be adsorbed on the coir pith at system pH 2 due to the electrostatic repulsion between Cr^{3+} and positively charged coir pith. Desorption and XANES indicated that most of the chromium bound on the coir pith was in Cr(III) form. This suggested that Cr(VI) could be adsorbed on coir pith by electrostatic attraction and subsequently toxic Cr(VI) could be reduced to less toxic Cr(III) on the coir pith surface. In addition, Fourier transform infrared (FT-IR) spectrometry analysis indicated that methoxy (O–CH$_3$) groups combined with aromatic ring and carbonyl (C=O) groups may be involved in the mechanism of chromium adsorption. The Cr(III) desorption was not complete (38.12–71.48%) although strong acid solutions such as 0.5 M HNO$_3$, 1 M HNO$_3$, 2 M HNO$_3$ were used as eluents. These results suggested that the reduced Cr(III) on the coir pith surface may be bound with C=O groups and O–CH$_3$ groups through coordinate covalent bonds in which a lone pair of electrons in the oxygen atoms

of the methoxy and carbonyl groups can be donated to form a shared bond with Cr(III). The Cr(III) bound with the carbonyl and methoxyl groups in coir pith by coordinated covalent bonds; therefore it was difficult to completely desorb the Cr(III).

4. Conclusions

Coir pith, a waste material from padding used in mattress factories, is an efficient adsorbent for Cr(VI) adsorption from electroplating wastewater. The "removal" percentage depended on the adsorbent dosage, contact time, temperature and system pH. However, the results indicated that Cr(VI) adsorption was greatly dependent upon the system pH. The highest Cr(VI) adsorption was 99.99% at system pH 2. The positive values of enthalpy change (ΔH) indicated an endothermic process. Desorption and XANES indicated that most of the chromium bound on the coir pith was in Cr(III) form due to the fact that the toxic Cr(VI) was easily reduced to less toxic Cr(III). The Cr(VI) adsorption on lignin extracted from coir pith confirmed that lignin was involved in the mechanism of chromium adsorption due to the high adsorption. Furthermore, FT-IR analysis indicated that carbonyl (C=O) groups and methoxy (O–CH$_3$) groups of lignin structure in coir pith may be involved in the mechanism of chromium adsorption. The reduced Cr(III) on the coir pith may be bound with carbonyl (C=O) groups and methoxy (O–CH$_3$) groups through a coordinate covalent bond. Therefore, it can be suggested that the mechanism of chromium adsorption involved a chemisorption process.

References

[1] N. Kungsricharoem, Application of electrochemical precipitation of treatment of Cr wastewater, Thesis, Asian Institute of Technology, Bangkok, 1994.
[2] Y.C. Sharma, Colloid Surf. A: Physicochem. Eng. Aspects 215 (2003) 155–162.
[3] A. Nakajima, Y. Baba, Water Res. 38 (2004) 2859–2864.
[4] M. Kobya, Bioresource Technol. 91 (2004) 317–321.
[5] S. Babel, T.A. Kurniawan, Chemosphere 54 (2004) 951–967.
[6] L. Chun, C. Hongzhang, L. Zuohu, Process Biochem. 39 (2004) 541–545.
[7] K. Ranganathan, Bioresource Technol. 73 (2000) 99–103.
[8] N.R. Bishnoi, M. Bajaj, N. Sharma, A. Gupta, Bioresource Technol. 91 (2004) 305–307.
[9] M. Dakiky, M. Khamis, A. Manassra, M. Meŕeb, Adv. Environ. Res. 6 (2002) 533–540.
[10] V.K. Gupta, M. Gupta, S. Sharma, Water Res. 35 (5) (2000) 125–1134.
[11] D.C. Sharma, C.F. Forster, Bioresource Technol. 47 (1994) 257–264.
[12] K. Selvi, S. Pattabhi, K. Kadirvelu, Bioresource Technol. 80 (2001) 87–89.
[13] N.K. Hamadi, X.D. Chen, M.M. Farid, M.G.Q. Lu, Chem. Eng. J. 84 (2001) 95–105.

[14] D. Daneshvar, D. Salari, S. Aber, J. Hazard. Mater. B 94 (2002) 49–61.

[15] K. Sevaraj, S. Manonmami, S. Pattabhi, Bioresource Technol. 89 (2003) 207–211.

[16] K. Mohanty, M. Jha, B.C. Meikap, M.N. Biswas, Chem. Eng. J. 117 (2006) 71–77.

[17] W. Stumm, J.J. Morgan, Aquatic Chemistry, 3rd ed., Wiley, New York, 1996, pp. 534–540.

[18] E. Kiefer, L. Sigg, P. Schosseler, Environ. Sci. Technol. 31 (1997) 759–764.

[19] Technical Association of the Pulp and Paper Industry, TAPPI Test Method, USA.

[20] Z. Reddad, C. Gerente, Y. Andres, P. Le Cloirec, Environ. Technol. 24 (2003) 257–264.

[21] D.D. Das, R. Mahapata, J. Pradhan, S.N. Das, R.S. Thakur, J. Colloid Interf. Sci. 232 (2000) 235–240.

[22] D.C. Sharma, C.F. Forster, Water SA 22 (2) (1996) 153–160.

[23] S. Deng, R. Bai, Water Res. 38 (2004) 2424–2432.

[24] M.X. Loukidou, A.I. Zouboulis, T.D. Karapantsios, K.A. Matis, Colloid Surf. A: Physiochem. Eng. Aspects 242 (2004) 93–104.

[25] A. Ozer, D. Ozer, Environ. Technol. 25 (2004) 689–697.

[26] K. Mohanty, M. Jha, B.C. Meikap, M.N. Biswas, Chem. Eng. Sci. 60 (2005) 3049–3059.

[27] D. Park, Y.-S. Yun, J.H. Jo, J.M. Park, Water Res. 39 (2005) 533–540.

[28] J.G. Parsons, M. Hejazi, K.J. Tiemann, J. Henning, J.L. Garsea-Torresdey, Microchem. J. 71 (2002) 211–219.

[29] J.L. Garsea-Torresdey, K.J. Tiemann, V. Armendariz, L. Bess-Obert, R.R. Chianelli, J. Rios, J.G. Parsons, G. Gamez, J. Hazard. Mater. B 80 (2000) 175–188.

[30] M.A. Khan, S.M. Ashraf, V.P. Maholtra, Int. J. Adhes. Adhes. 24 (2004) 485–493.